



Delft University of Technology

## Loss evaluation of GaN GIT in a high frequency boost converter in different operation modes

Wang, Wenbo; Pansier, Frans; Popovic, Jelena; Ferreira, J. A.

### Publication date

2016

### Document Version

Final published version

### Published in

CIPS 2016 - 9th International Conference on Integrated Power Electronics Systems

### Citation (APA)

Wang, W., Pansier, F., Popovic, J., & Ferreira, J. A. (2016). Loss evaluation of GaN GIT in a high frequency boost converter in different operation modes. In *CIPS 2016 - 9th International Conference on Integrated Power Electronics Systems* (pp. 1-6). VDE Verlag GMBH.  
<https://ieeexplore.ieee.org/abstract/document/7736742>

### Important note

To cite this publication, please use the final published version (if applicable).  
Please check the document version above.

### Copyright

Other than for strictly personal use, it is not permitted to download, forward or distribute the text or part of it, without the consent of the author(s) and/or copyright holder(s), unless the work is under an open content license such as Creative Commons.

### Takedown policy

Please contact us and provide details if you believe this document breaches copyrights.  
We will remove access to the work immediately and investigate your claim.

# Loss evaluation of GaN GIT in a high frequency boost converter in different operation modes

Wenbo Wang, Frans Pansier, Jelena Popovic, J.A. Ferreira  
Delft University of Technology, The Netherlands

## Summary

In this paper, losses in a 600V Gallium Nitride (GaN) Gate Injection Transistor (GIT) were evaluated in different operation modes of a boost converter. Analytical loss model of GaN GIT, in which circuit and package parasitics are accounted for, was developed to assist the evaluation. Losses in GIT were assessed in a boost converter using the model and the results showed that: in Continuous Conduction Mode (CCM) and Boundary Conduction Mode (BCM), turn-on loss, mainly originated from discharging of transistor output capacitance, dominates in GIT; in Boundary Conduction Mode with Valley Switching (BCM-VS), where transistor is switched on with reduced voltage and zero current, turn-on loss can be greatly reduced. In BCM-VS, where turn-off current is higher than CCM and BCM, turn-off loss dominates as  $C_{gd}$  is large and the ratio between  $C_{ds}$  and  $C_{gd}$  is small in low voltage range. Experiments were performed to validate the loss model at both 100kHz and 1MHz as well as to prove and demonstrate the loss analysis.

## 1. Introduction

High frequency power conversion is an ongoing trend in power electronics. To achieve high frequency operation while maintaining high efficiency, suitable switching devices are required. GaN power semiconductors, resulting from their material properties, have faster switching speed than Silicon (Si) counterparts and are recognized as one of the good candidates to replace Si devices [1][2]. Up to date, performances of different types of GaN HEMTs were evaluated, and the results showed that GaN HEMTs are promising for high frequency applications under soft turn-on conditions [3][4].

In this paper, losses in a new type of GaN transistor, GaN GIT from Panasonic, are evaluated in a boost converter. Analytical loss model of GIT is developed as a tool to predict transistor losses when it is operated in different modes i.e. different switching conditions. Experimental measurements are conducted to validate the model and to prove the analysis.

## 2. Loss modeling and analysis of GaN GIT in a boost converter

### 2.1 Analytical loss modeling of GaN GIT in a boost converter

To evaluate performances of GaN GIT, loss modeling of the device is needed. Loss models of GaN HEMTs had been well developed, whereas loss modeling of GaN GIT, to our knowledge, has not been performed. In this paper, losses in

GaN GIT is modeled and analyzed in a boost converter. Unlike the approach recommended by Panasonic, GIT is drove with no auxiliary circuit in gate loop in this paper [5].

#### 2.1.1 Loss modeling approach

An equivalent circuit of a GaN GIT based boost converter that includes circuit and package parasitic inductances (drain inductance  $L_d$ , gate inductance  $L_g$  and common source inductance between gate loop and switching loop  $L_s$ ) as well as parasitic capacitances (parasitic capacitances of the transistor:  $C_{gd}$ ,  $C_{gs}$  and  $C_{ds}$ ) that has been proved to have major effects on transistor switching characteristics in a diode-clamped, inductive load switching circuits [3][6][7] is shown in Fig 1. It should be noted that  $L_d$  consists of inductance of transistor package at drain terminal  $L_{d-GIT}$  and inductance of PCB at drain side  $L_{d-PCB}$ , and so does  $L_g$  and  $L_s$ . Inductance in the rest part of commutation loop (lumped as  $L_D$ ) and mutual inductances between different leads of GIT ( $M_{gs}$ ,  $M_{gd}$ ,  $M_{ds}$ ) are also included. Nonlinear properties of  $C_{gd}$  and  $C_{ds}$  in GIT and  $C_D$  in the freewheeling diode are accounted for. Reverse recovery effect of the freewheeling diode is not considered as it is avoided in some operation modes (e.g. BCM and BCM-VS) and, in the mode (e.g. CCM) where the effect is critical, Silicon Carbide (SiC) diode that has no reverse recovery charge, will be used.

#### 2.1.2 Loss modeling of GaN GIT in a boost converter in CCM

Switching transients of GaN GIT are divided into different stages and sub-stages, as characterized

for switching behaviors of both GaN HEMTs and Si MOSFET [3][4][6][7]. Values of parasitic elements are modeled differently according to the conditions such as  $v_{ds}$  variation range, current direction in GaN GIT package leads, etc. in each single stage or substage.

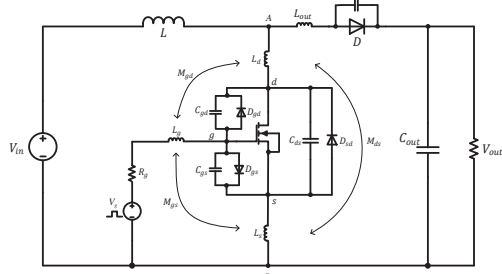


Fig.1 GaN GIT based boost converter with circuit and package parasitics

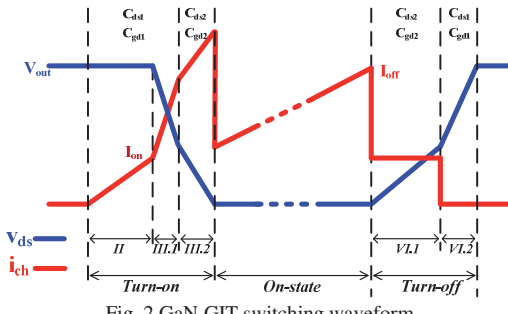


Fig. 2 GaN GIT switching waveform

$$\begin{aligned} C_{ds1} &= C_{ds}(V_{out}), \quad C_{gd1} = C_{gd}(V_{out}), \quad C_{d2} = C_{D(V_{out})} \\ C_{ds2} &= \frac{C_{ds}(V_{out}) + C_{ds}(R_{ds-on}I_{on})}{2}, \quad C_{gd2} = \frac{C_{gd}(V_{out}) + C_{gd}(R_{ds-on}I_{on})}{2} \\ C_{D1} &= \frac{C_D(V_{out}) + C_D(0)}{2} \end{aligned}$$

#### A. Turn-on transient

##### Stage I Turn-on delay

When gate voltage  $V_g$  is initiated, the resulting gate current in the gate loop starts to charge the input capacitance  $C_{gs}$  and  $C_{gd}$ . As  $C_{gs}$  is usually much larger than  $C_{gd}$  when  $v_{ds}$  is high, it is assumed that only  $C_{gs}$  is charged in this stage [3][6]. Before transistor threshold voltage  $V_{th}$  is reached, status of power stage doesn't change, and therefore no power loss is generated in GaN GIT. At the end of this stage,  $V_{gs}$  equals  $V_{th}$ .

##### Stage II Channel current rise

Once  $V_{th}$  is reached, channel of the GIT becomes conductive, GIT operates in saturation region as  $v_{ds} > v_{gs} - V_{th}$ . Therefore, maximum current the channel can conduct is determined by  $v_{gs}$ . Due to time-changing current that flows in the commutation loop, voltage drop on parasitic inductances will be induced, affecting  $v_{ds}$  and losses in the transistor.

$$i_{ch-ir}(t) = i_{L_d}(t) - i_{C_{ds}}(t) - i_{C_{dg}}(t) \quad (1)$$

$$i_{ch-ir}(t) = g_{fs}(v_{gs}(t) - V_{th}) \quad (2)$$

By solving the equations from both gate loop and commutation loop, values of transistor channel current and voltage on the transistor i.e. instant power loss in GaN GIT can be obtained, though the expressions are quite complex. In this paper, channel current is considered as equal to drain terminal current  $i_{L_d}(t)$  in this stage; variation of  $v_{ds}$  is accounted for by adding loss of discharging GaN GIT output capacitance. At the end of this stage, transistor channel takes over the whole load current  $I_{on}$  and voltage on GIT is  $V_{ds(t_{ir})}$ . Switching loss in this stage is modeled as:

$$P_{lr} = f_{sw} \int_0^{t_{ir}} v_{ds}(t) i_{L_d}(t) dt + \frac{C_{ds1} + C_{gd1}}{2} (V_{out}^2 - V_{ds(t_{ir})}^2) f_{sw} \quad (3)$$

Where  $t_{ir}$  denotes current rise time and  $f_{sw}$  is the operation frequency of the converter.

##### Stage III Voltage fall

After GaN GIT has taken over  $I_{on}$ , the freewheeling diode stops conducting and blocks output voltage  $V_{out}$ . Voltage on transistor starts to fall,  $C_{ds}$  and  $C_{gd}$  get discharged through transistor channel. As GIT is still working in saturation region, the current through GIT channel is still controlled by  $v_{gs}$ . As indicated from datasheet of GIT, values of  $C_{ga}$  and  $C_{ds}$  are almost constant when  $v_{ds}$  is greater than 255 V. Below 255 V, however, both capacitance values vary with  $v_{ds}$ , and  $C_{gd}$  varies dramatically. To more accurately model loss, this stage is divided into two substages according to the value of  $v_{ds}$ .

##### Substage III.1 High voltage range

As drain current is constant ( $I_{on}$ ),  $M_{gd}$  and  $M_{ds}$  are modelled as zero. Rearranging equations for Stage II with modifications on values of channel current and mutual inductances, expressions of channel current  $i_{ch-vf1}(t)$  and drain source voltage  $v_{ds-vf1(t)}$  can be obtained. This stage ends when  $v_{ds}$  drops from  $V_{ds(t_{ir})}$  to 255 V by the time  $t_{vf1}$ . Loss in this stage is modelled as

$$P_{vf1} = f_{sw} \int_0^{t_{vf1}} v_{ds-vf1(t)} i_{ch-vf1}(t) dt \quad (4)$$

##### Substage III.2 Low voltage range

In low  $v_{ds}$  range, nonlinearity of parasitic capacitances should be accounted for. The relationships between capacitance values and  $v_{ds}$  can be modeled through curve fitting to find polynomial expressions of  $C_{gd}$  and  $C_{ds}$  as functions of  $v_{ds}$ . Although this approach could result in accurate calculation of loss, as  $C_{gd}$  and  $C_{ds}$  are coupled with the time changing  $v_{ds}$ , it usually ends up with complex equations and

therefore calls for simplifications [4]. In this work, average values of  $C_{gd}$  and  $C_{ds}$  are used to account for nonlinearity of the capacitances.

After a fall time of  $t_{vf2}$ ,  $v_{ds}$  decrease to  $R_{ds-on}I_{on}$  and this stage ends. Expressions of channel current  $i_{ch-vf2}(t)$  and voltage  $v_{ds-vf2}(t)$  can be obtained by substituting values of  $C_{gd}$  and  $C_{ds}$  with  $C_{gd2}$  and  $C_{ds2}$ , replacing  $i_{L_d}$  with  $I_{on}$  and, as drain current is constant, setting  $M_{gd}$ ,  $M_{ds}$  to zero in equations in previous stage. Loss in GIT in this substage:

$$P_{vf2} = f_{sw} \int_0^{t_{vf2}} v_{ds-vf2}(t) i_{ch-vf2}(t) dt \quad (5)$$

Parasitic capacitance of the freewheeling diode will be charged during transistor voltage fall and the corresponding current will flow through transistor channel. The displacement-current induced loss is accounted for by:

$$P_{CD-dis} = \frac{Q_{V_{out}} V_{out}}{2} f_{sw} \quad (6)$$

$Q_{V_{out}}$  is the charge needed to build potential across the diode up to  $V_{out}$  and value of  $Q_{V_{out}}$  can be obtained from diode datasheet. After  $v_{ds}$  drops to  $R_{ds-on}I_{on}$ ,  $v_{gs}$  continues to increase and, as gate-source characteristics is modeled as a capacitor in parallel with a diode (forward voltage  $V_{gsD}$ , on-state resistance  $R_{gsD}$ ), final value of  $v_{gs}$  is determined by:

$$V_{gson} = V_{gsD} + \frac{V_g - V_{gsD}}{R_{gon} + R_{gsD}} R_{gsD} \quad (7)$$

Because of the large transconductance  $g_{fs}$  of the transistor, the gate-source diode illustrated in Fig. 1, will not conduct during switching transient until the channel current reaches about 40A. And thus, the effect of gate-source diode on turn-on loss is not considered in this paper.

#### B. Turn-off transient

##### Stage V Turn-off delay

When  $V_g$  starts decreasing,  $C_{gs}$  and  $C_{gd}$  are discharged and turn-off transient starts. As  $v_{gs}$  will firstly drop to  $V_{gsD}$  under the influence of gate-source diode and then falls without the effects of the diode, two substages exist.

##### Substage V.1 Gate-source diode in on-state

In this substage, gate source voltage drops from  $V_{gson}$  to  $V_{gsD}$  by the time  $t_{offd1}$ .

$$i_{gs}(t) = C_{gs} \frac{dv_{gs}(t)}{dt} + \frac{V_g - V_{gsD}}{R_{gsD}} \quad (8)$$

##### Substage V.2 Gate-source diode in off-state

After the gate-source diode stops conducting,  $v_{gs}$  drops from  $V_{gsD}$  to turn-off plateau voltage  $V_{gs-vr}$ , with a time duration of  $t_{offd2}$ .

As channel current and drain source voltage of

GaN GIT remains the same as when transistor is in on-state, this stage can be regarded as an extension of transistor on-state. Power loss in GaN GIT during this stage is estimated as:

$$P_{offdelay} = R_{ds-on} I_{off}^2 (t_{offd1} + t_{offd2}) f_{sw} \quad (9)$$

##### Stage VI Voltage rise

Theoretically, after the delay stage, transistor will not enter into saturation region until  $v_{ds} > v_{gs} - V_{th}$ . Given the fact that GaN GIT has a large  $g_{fs}$ , transition time from ohmic region to saturation is neglected [6]. During voltage rise, load current  $I_{off}$  splits into four parts:  $i_{C_{gd}}$  that charges  $C_{gd}$ , which equals the gate current;  $i_{C_{ds}}$  that charges  $C_{ds}$ ;  $i_{C_D}$  that charges  $C_D$  and  $i_{ch}$  that flows through transistor channel. It is assumed that  $v_{gs}$  stays constant at  $V_{gs-vr}$  in this stage:

$$I_{off} = I_{C_{dg}} + I_{C_{ds}} + I_{ch} + I_C \quad (10)$$

$$I_{C_{dg}} = C_{gd3} \frac{dv_{dg}(t)}{dt} = \frac{V_{gs-vr}}{R_{goff}} \quad (11)$$

$$I_{ch} = g_{fs} (V_{gs-vr} - V_{gs-th}) \quad (12)$$

$V_{gs-vr}$  is determined by applying values of  $C_{gd}$  and  $C_{ds}$  when drain source voltage is  $R_{ds-on}I_{on}$ :

$$C_{ds3} = C_{ds(R_{ds-on}I_{on})}, C_{gd3} = C_{gd(R_{ds-on}I_{on})}$$

As discussed in Stage III, values of parasitic capacitors in GaN GIT show different characteristics below and above 255 V of  $v_{ds}$ . To account for this effect, this stage is separated into two substages as well.

##### Substage VI.1 Low voltage range

In low voltage range, averaged capacitance values are used:

$$v_{ds-vr1}(t) = \frac{V_{gs-vr}}{R_{goff} C_{gd2}} t \quad (13)$$

$$\begin{cases} I_{ch-vr1} = \\ I_{off} - \frac{V_{gs-vr}}{R_{goff}} \left( 1 + \frac{C_{ds2} + C_{D2}}{C_{gd2}} \right), \quad I_{off} > \frac{V_{gs-vr}}{R_{goff}} \left( 1 + \frac{C_{ds2} + C_{D2}}{C_{gd2}} \right) \\ 0, \quad I_{off} \leq \frac{V_{gs-vr}}{R_{goff}} \left( 1 + \frac{C_{ds2} + C_{D2}}{C_{gd2}} \right) \end{cases} \quad (14)$$

This stage ends when  $v_{ds}$  reaches 255 V. Loss generated in GIT in this substage is calculated as:

$$P_{vr1} = f_{sw} \int_0^{t_{vr1}} v_{ds-vr1}(t) I_{ch-vr1} dt \quad (15)$$

$t_{vr1}$  stands for the time needed in this substage.

##### Substage VI.2 High voltage range

In high voltage range,  $v_{ds-vr2}(t)$  varies different with time than its counterpart in low voltage range and the value of channel current  $I_{ch-vr2}$  is also not the same as  $I_{ch-vr1}$ . Expressions of  $I_{ch-vr2}$  and  $v_{ds-vr2}(t)$  can be obtained by substituting  $C_{gd2}$ ,  $C_{ds2}$  and  $C_{D2}$ , in (13) and (14) with  $C_{gd1}$ ,  $C_{ds1}$  and  $C_{D1}$  respectively. After a time of  $t_{vr2}$ ,  $v_{ds}$  reaches  $V_{out}$ . Loss occurred in GaN GIT during this stage can be expressed as:

$$P_{vr2} = f_{sw} \int_0^{t_{vr2}} v_{ds-vr2}(t) I_{ch-vr2} dt \quad (16)$$

#### Stage VII Drain current fall

After  $v_{ds}$  increased up to  $V_{out}$ , diode begins to conduct, load current commutes from transistor to diode. Analytical loss modeling approach of GaN GIT in this stage is the same as the modeling of corresponding stage of GaN HEMT in [3]. It should be noted that during drain current fall, considering the current directions in this stage, coupling coefficients are different from the values in turn-on transient.

#### C. Conduction loss

Apart from the switching losses, there is also conduction loss, which is generated during GaN GIT on stage

$$P_{cond} = I_{rms-on}^2 R_{ds-on} \quad (17)$$

In case of reverse conduction, loss can be estimated as

$$P_{cond-rev} = f_{sw} \int_0^{t_{rev}} v_{ds-rev}(t) i_{Ld-rev}(t) dt \quad (18)$$

Where  $v_{ds-rev}$  and  $i_{Ld-rev}$  are voltage on and current through the transistor, respectively. And  $t_{rev}$  is the duration of reverse conduction.

## 2.2 Operation modes in a boost converter

Apart from the commonly seen operation modes of a boost converter, CCM, DCM and BCM, a mode of so-called BCM-VS, which is commonly used in PFC boost converters, also exists [9]-[11]. As explained in detail in [3], in BCM-VS, transistor will be switched on at reduced voltages with Zero current (ZCS) and therefore turn-on loss can be minimized.

Different switching conditions for GIT are enabled by operating the GIT based boost converter in different modes: in CCM, turn-on process is hard switching; in BCM, ZCS turn-on can be achieved, the effect of turn-on current on turn-on loss is excluded; in BCM-VS, ZCS turn-on can be maintained while the voltage across the switch is at a low value (or even zero).

## 2.3 Loss analysis of GaN GIT in different operation modes

### 2.3.1 Loss breakdown and analysis

Utilizing the developed model, losses in GaN GIT were analysed in three different operation modes at 1MHz, with an output voltage of 400V and a power of 300W with the specifications detailed in Table III in a boost converter. As illustrated in Fig. 3: in CCM, turn-on loss dominates (99.4%), while turn-off loss is zero; in

BCM, where turn-on loss is caused only by discharging transistor output capacitance, turn-on loss still dominates (73.2%), turn-off loss contributes 25.8% to total loss; in BCM-VS I ( $V_{out} < 2V_{in}$ ), where GIT will be switched on with ZCS at 120V and turned off with similar current as BCM, turn-on loss is greatly reduced while turn-off dominates (70.5%); in BCM-VS II ( $V_{out} > 2V_{in}$ ), where GIT is to be switched on with ZCS and negligible voltage, turn-off loss is up to 94.4% of total loss; conduction losses are low in all modes resulting from the low on-state resistance of less than  $0.1\Omega$ .

Table I. Specifications and losses in the boost converter in different modes

| Mode      | $v_{in}$ (V) | $I_{on}$ (A) | $I_{off}$ (A) | Loss (W) |
|-----------|--------------|--------------|---------------|----------|
| CCM       | 200          | 1.35         | 1.65          | 12.33    |
| BCM       | 200          | 0            | 3             | 10.98    |
| BCM-VS I  | 260          | 0            | 3.2           | 4.66     |
| BCM-VS II | 120          | 0            | 6.6           | 10.76    |

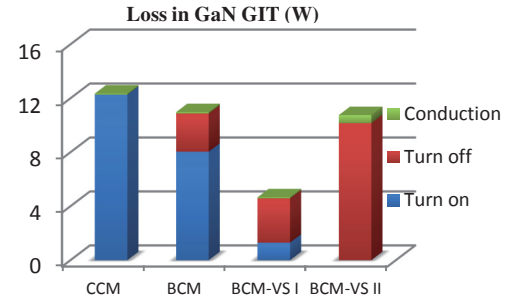


Fig. 3 Loss breakdown of GIT in different modes

The results of loss breakdown indicate that: in CCM and BCM, turn-on loss dominates in GaN resulting from the discharging of the large output capacitance of the transistor; in BCM-VS I and BCM-VS II, where transistor is to be switched on at reduced voltage and switched off with higher current, turn-off loss dominates. The high turn-off loss is due to the facts that  $C_{gd}$  is large and the ratio between  $C_{ds}$  and  $C_{gd}$  is small in low voltage range in GIT, which will end up with long voltage rise time and large channel current. Turn off loss, as implied in equations 13 and 14, can be reduced by paralleling external capacitors to GaN GIT, reducing gate resistance  $R_{g-off}$  or enforcing negative  $v_{gs}$ .

### 2.3.2 Effects of parasitic inductances on switching loss

Effects of parasitic inductances on switching loss of GaN GIT depend greatly on operation modes the transistor is working in. In BCM, BCM-VS I

and BCM-VS II, where GaN GIT is switched on with ZCS, parasitic inductances has no effects on turn-on loss. As implied by (14), loss will be generated in substage VI.1 if there's current in GIT channel. As the ratio between  $C_{ds}$  and  $C_{gd}$  increases up to a value of 70 after  $V_{ds}$  exceeds 255V, no channel current will be present unless the turn-off current is larger than 49.3A in substage VI.2. And therefore, turn-off loss is not influenced by parasitic inductances.

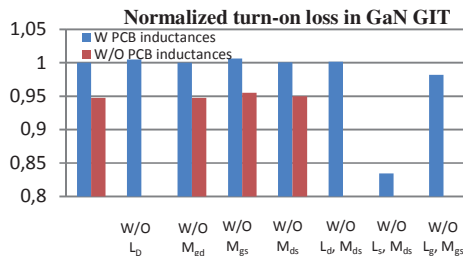


Fig.4 Effects of parasitic inductances in CCM on turn-on loss

The effects of different parasitic inductances on turn-on loss in CCM are demonstrated in Fig. 4.  $L_s$  has the largest influence on turn-on loss in CCM because it behaves as a negative feedback between gate loop and switching loop and thus slows down switching transients.  $L_D$ ,  $L_d$  and  $M_{ds}$  lower turn-on loss by reducing the value of  $v_{ds}$ . During turn-on, the presence of  $L_g$  increases turn-on loss, which differs from the conclusion that  $L_g$  affects only delay times but not loss in [6]. Coupling effect between gate and source ( $M_{gs}$ ) helps to reduce effective inductances in common source and gate, and decrease turn-on loss thereof. Apart from  $L_g$ , the rest parasitic inductances have limited effects on turn-on loss.

The effects of mutual inductances on turn-on loss are further illustrated by considering only package inductances i.e. setting values of  $L_{d-PCB}$ ,  $L_{s-PCB}$ , and  $L_{g-PCB}$  to zero. The influences of mutual inductances are enhanced although still limited. For instance, when PCB inductances present, existence of  $M_{gs}$  and  $M_{ds}$  would reduce 0.64% and 0.08% of turn-on loss, respectively, while when there's no PCB inductances on drain, source and gate exist, the values grows to 7.84% and 2.59%, respectively.

### 3. Experimental results

A 300W boost converter prototype is built to perform loss model validation and assess losses in GaN GIT in different operation modes. Losses in GIT are measured thermally. The effects of diode on transistor temperature may be excluded

by proper layout i.e. putting the diode physically away from the transistor; while the effect of driver on transistor temperature can be omitted as losses in the driver was negligible given the low driving voltage of 4V and the fact that GIT requires only 8 nC to be fully on. Experimental verifications were performed and confirmed that both diode and driver have negligible contribution to temperature increase of GIT. A lookup table that calibrates relationship between loss and temperature increase in GIT was made by injecting different values of DC current into GIT when it is kept in on-state. With help of the look-up table, losses in GIT are quantified.

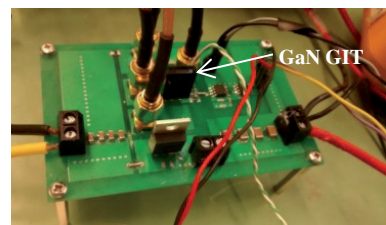


Fig.5 Converter prototype employing GaN GIT

#### 3.1 Loss model validation

The loss model was validated experimentally in CCM at 100 kHz. The validations were performed using the prototype shown in Fig.5 with the specifications detailed in Table II. Circuit and package parasitic inductances were calculated by PEEC (Partial Element Equivalent Circuit) tool and values of parasitic capacitances of the transistor were extracted from transistor datasheet. SiC Schottky diode was used to eliminate boost diode's reverse recovery current. As indicated in Fig. 6, the modelled loss agreed well with measurement results.

Table II. Values of parasitic elements

| Parasitics |             | Values | Parasitics |             | Values |
|------------|-------------|--------|------------|-------------|--------|
| $L_d$      | $L_{d-PCB}$ | 1.40nH | $L_s$      | $L_{s-PCB}$ | 1.97nH |
|            | $L_{d-GIT}$ | 1.73nH |            | $L_{s-GIT}$ | 1.81nH |
| $L_g$      | $L_{g-PCB}$ | 2.64nH | $C_{gd1}$  | $C_{gd2}$   | 1.1pF  |
|            | $L_{g-GIT}$ | 1.81nH |            |             | 22.1pF |
| $M_{gs}$   |             | 0.29nH | $C_{gd3}$  |             | 43pF   |
| $M_{gd}$   |             | 0.54nH | $C_{ds1}$  |             | 70pF   |
| $M_{ds}$   |             | 0.54nH | $C_{ds2}$  |             | 145pF  |
| $L_D$      |             | 9.87nH | $C_{ds3}$  |             | 220pF  |
| $C_{gs}$   |             | 270pF  | $C_{D1}$   |             | 27pF   |
| $Q_{out}$  |             | 5nC    | $C_{D2}$   |             | 12pF   |

Table III. Specifications of converter test points

| $P_{out}$ (W) | $v_{out}$ (V) | $I_{on}$ (A) | $I_{off}$ (A) |
|---------------|---------------|--------------|---------------|
| 20            | 100           | 0.35         | 0.44          |
| 45            | 150           | 0.51         | 0.65          |
| 75            | 200           | 0.70         | 0.88          |

|     |     |      |      |
|-----|-----|------|------|
| 120 | 250 | 0.87 | 1.09 |
| 170 | 300 | 1.04 | 1.31 |
| 230 | 350 | 1.20 | 1.52 |
| 300 | 400 | 1.40 | 1.70 |

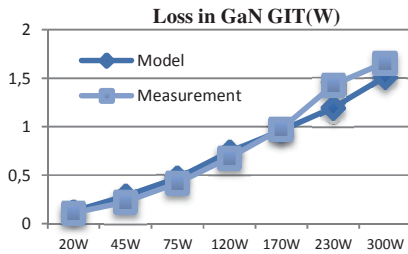


Fig. 6 Measured and calculated (modeled) loss in GaN GIT

### 3.2 Loss evaluation of GIT at 1 MHz in different operation modes

In CCM, GaN GIT is hard switched in both turn-on and turn-off with low currents, measured loss is 11.9W. In BCM, the transistor is switched on with ZCS and off with higher current than CCM, loss is measured as 11W. In BCM-VS I and BCM-VS II, ZCS turn-on are maintained while turn-on voltages are reduced and turn-off currents are larger than BCM, losses in GaN GIT are measured as 4.5W and 9.8W, respectively. Measurement results agree well with the analysis in Section 3.2.1, although there are deviations in values. The measured and calculated loss of GaN GIT at 1MHz also proved that the model can predict loss in GaN GIT with satisfactory accuracy. Deviations originate mainly from measurement errors and inaccurate modeling of capacitance during turn-off.

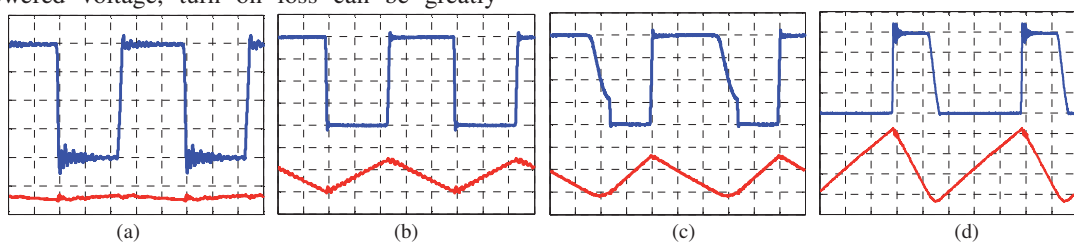
## 4. Conclusions

In this paper, loss model of a 600V GaN GIT was developed. Losses in GIT were then evaluated in a boost converter in three different operation modes-CCM, BCM and BCM-VS utilizing the loss model. It is shown that in CCM and BCM, turn-on loss dominates originating from discharging of the large output capacitance. In BCM-VS, where GIT is switched on with lowered voltage, turn on loss can be greatly

reduced. It was revealed that the ratio of  $C_{ds}/C_{gd}$ , which affect turn-off loss, is low in GaN GIT in low  $v_{ds}$  range (below 255V) and therefore, in BCM (with high current) and in BCM-VS, where turn-off current is much larger than CCM, turn-off loss dominates. Given these facts, losses in BCM-VS can be reduced by improving driving circuit (e.g. adding auxiliary circuits) or paralleling external capacitors to drain-source of GIT. As with CCM and BCM (with low current), reduction of the parasitic capacitance e.g. die shrinking is needed to decrease the loss. Conduction is low in all modes resulting from the low on-state resistance of GaN GIT. Experiments were performed to validate the loss mode and to prove the analysis.

## References

1. M.A. Khan, G. Simin, S.G.Pytel, A.Monti, E. Santi, J.L.Hudgins, "New Development in Gallium Nitride and the Impact on Power Electronics" Power Electronics Specialists Conference, 2005, PESC'05, IEEE 36<sup>th</sup>, vol., no., pp.15-26, 16-16 June 2005
2. J. Popovic; J.A. Ferreira; J.D.van Wyk; F. Pansier, "System Integration of GaN Converters- Paradigm Shift, challenges and opportunities", 8th International Conference on Integrated Power Systems (CIPS), Feb, 2014
3. W. Wang; F. Pansier; J. Popovic; J.A. Ferreira, "Optimal Utilization of Low Voltage GaN HEMT in High Frequency Boost Converter", 9th International Conference on Power Electronics-ECCE Asia (ICPE 2015-ECCE Asia), June, 2015
4. X. Huang, Q. Li, Z. Liu, and F. C. Lee, "Analytical loss model of high voltage GaN HEMT in cascode configuration," IEEE Trans. Power Electron., vol. 29, no. 5, pp. 2208–2219, May 2014
5. GIT driving method, Panasonic
6. J. Wang, H. S. Chung, and R. T. Li, "Characterization and experimental assessment of the effects of parasitic elements on the MOSFET switching performance," IEEE Trans. Power Electron., vol. 28, no. 1, pp. 573–590, Jan. 2013.
7. Yuancheng Ren, Ming Xu, Jinghai Zhou, and Fred Lee, "Analytical Loss Model of Power MOSFET", IEEE Transactions on Power Electronics, Vol. 21, No. 2, March 2006, pp 310–319
8. Y. Uemoto, M. Hikita, H. Ueno, H. Matsuo, H. Ishida, M. Yanagihara, T. Ueda, T. Tanaka, and D. Ueda, "Gate injection transistor (GIT)—A normally-off AlGaN/GaN power transistor using conductivity modulation," IEEE Trans. Electron Devices, vol. 54, no. 12, pp. 3393–3399, Dec. 2007.
9. Laszlo Huber, Brian T. Irving, Milan M. Jovanovic "Effects of Valley Switching and Switching –Frequency Limitation on Line-Current Distortions of DCM/CCM Boundary Boost PFC Converters" IEEE Transaction on Power Electronics, Vol.24, NO.2 pp339-347, Feb,2009
10. Onsemi, " Power Factor Correction(PFC) Handbook" [www.onsemi.com/pub\\_link/Collateral/HBD853-D.PDF](http://www.onsemi.com/pub_link/Collateral/HBD853-D.PDF)
11. PFC controller TEA 1750 Datasheet [www.nxp.com/documents/data\\_sheet/TEA1750.pdf](http://www.nxp.com/documents/data_sheet/TEA1750.pdf)
12. Gecko EMC [www.geckosimulations.com](http://www.geckosimulations.com)
13. GaN GIT(600V, 15A) datasheet, Panasonic

Fig. 7 Measurement results: (a) CCM; (b) BCM; (c) BCM-VS I ( $V_{out} < 2V_{in}$ ); (d) BCM-VS II ( $V_{out} > 2V_{in}$ )  
( $V_{ds}$ : 200V/Div;  $i_L$ : 2A/Div; time: 200ns/Div)